Consideration of Moving Tooth Load in Gear Crack Propagation Predictions

David G. Lewicki, Lisa E. Spievak, Paul A. Wawrzynek,
Anthony R. Ingraffea and Robert F. Handschuh

David G. Lewicki

is a senior aerospace engineer with the U.S. Army Research Laboratory at NASA's Glenn Research Center in Cleveland, OH. He has been involved in gear crack propagation research, as well as transmission life and reliability predictions and gear dynamics predictions. He also has worked on low-noise, high-strength spiral bevel gears; face gears for helicopter drive systems; lubricants; and diagnostics. He has written or co-written more than 70 technical articles in the field of drive systems.

Lisa E. Spievak

is a structural engineer in the design and analysis group of ATA Engineering Inc., located in San Diego, CA. She is an expert in applying computer techniques to design, analyze and test highly stressed structures and in interpreting fracture and fatigue requirements for those structures. As a graduate student, she performed research with the Cornell Fracture Group in which she simulated three-dimensional fatigue crack growth in spiral bevel gears.

Introduction

Effective gear designs balance strength, durability, reliability, size, weight, and cost. Even effective designs, however, can have the possibility of gear cracks due to fatigue. In addition, truly robust designs consider not only crack initiation, but also crack propagation trajectories. As an example, crack trajectories that propagate through the gear tooth are the preferred mode of failure compared to propagation through the gear rim. Rim failures will lead to catastrophic events and should be avoided. Analysis tools that predict
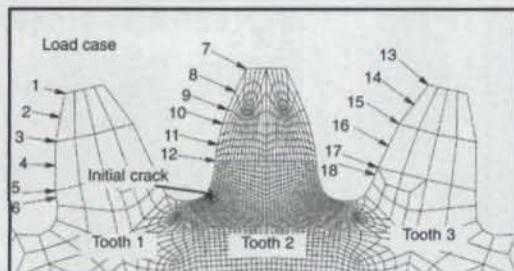

Figure 1—Location of load cases for finite element mesh.

Figure 2—Mode I and mode II stress intensity factors for a unit load and an initial crack of 0.26 mm.

crack propagation paths can be a valuable aid to the designer to prevent such catastrophic failures.

Pertaining to crack analysis, linear elastic fracture mechanics applied to gear teeth has become increasingly popular. The stress intensity factors are the key parameters to estimate the characteristics of a crack. Analytical methods using weight-function techniques to estimate gear tooth stress intensity factors have been developed (Refs. 1 and 17). Numerical techniques, such as the boundary element method and finite element method, have also been studied (Refs. 12 and 21). Based on stress intensity factors, fatigue crack growth and gear life predictions have been investigated (Refs. 2, 3, 5 and 9). In addition, gear crack trajectory predictions have been addressed in a few studies (Refs. 6, 7, 13, 14 and 19).

From publications on gear crack trajectory predictions, the analytical methods have been numerical (finite element method or boundary element method) while solving a static stress problem. In actual gear applications, however, the load moves along the tooth, changing in both magnitude and position. No work has been done investigating the effect of this moving load on crack trajectories.

The objective of the current work is to study the effect of moving gear tooth load on crack propagation predictions. Two-dimensional analysis of an involute spur gear using the finite element method is discussed. Also, three-dimensional analysis of a spiral-bevel pinion gear using the boundary element method is discussed. A quasi-static numerical simulation method is presented in which the gear tooth engagement is broken down into multiple load steps, with each step analyzed separately. Methods to analyze the steps are discussed, and predicted crack shapes are compared to experimental results.

Two-Dimensional Analysis

Gear Modeling. The two-dimensional analysis was performed using the FRANC (FRacture ANalysis Code) computer program developed by
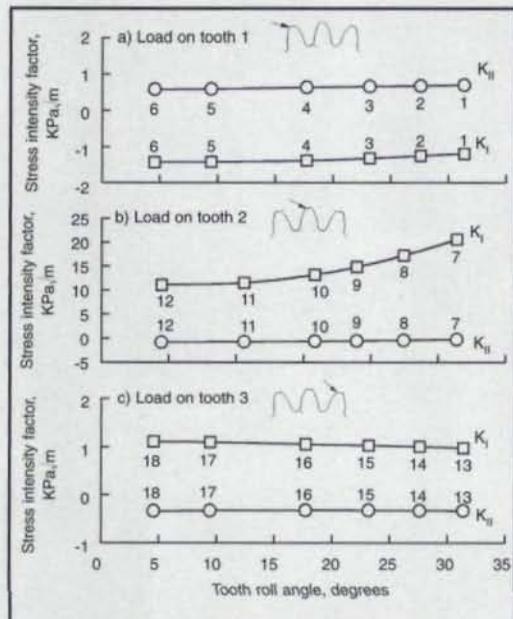
Wawrzynek (Ref. 23). The program is a general-purpose finite element code for the static analysis of two-dimensional cracked structures. The program uses principles of linear elastic fracture mechanics and is capable of analyzing plane strain, plane stress, or axi-symmetric problems. A unique feature of the program is the ability to model cracks and crack propagation in a structure. A rosette of quarter-point, six-node, triangular elements is used around the crack tip to model the inverse square-root stress singularity. Mode I and mode II stress intensity factors, K_I and K_{II} respectively, can be calculated using a variety of methods. (As a refresher, mode I loading refers to loads applied normal to the crack plane and tends to open the crack. Mode II refers to in-plane shear loading.) The stress intensity factors quantify the state of stress in the region near the crack tip. In the program, the stress intensity factors can be used to predict the crack propagation trajectory angles, again using a variety of methods. In addition, the program has a unique re-meshing scheme to allow automated processing of the crack simulation.

A spur gear from a fatigue test apparatus was modeled to demonstrate the two-dimensional analysis. The modeled gear had 28 teeth, a 20° pressure angle, a module of 3.175 mm (diametral pitch of 8/in.), and a face width of 6.35 mm (0.25 in.). The gear had a backup ratio (defined as the rim thickness divided by the tooth height) of 3.3. The complete gear was modeled using mostly 8-node, plane stress, quadrilateral finite elements. For improved accuracy, the mesh was refined on one of the teeth in which a crack was inserted. The total model had 2,353 elements and 7,295 nodes. Four hub nodes at the gear inner diameter were fixed to ground for boundary conditions. The material used was steel.

Tooth Loading Scheme. To determine the effect of gear tooth moving load on crack propagation, the analysis was broken down into 18 separate load cases (Fig. 1). An initial crack of 0.26 mm (0.010 in.) in length was placed in the fillet of tooth 2, normal to the surface, at the location of the maximum tensile stress (uncracked condition). Six load cases were analyzed separately with the load on the tooth ahead of the cracked tooth, six on the cracked tooth, and six on the tooth after the cracked tooth. The calculated stress intensity factors for unit loads at each of the load positions are shown in Figure 2. These stress intensity factors were calculated using the J-integral technique (Ref. 20). Loads on tooth 2 (cracked tooth) produced tension at the crack tip.
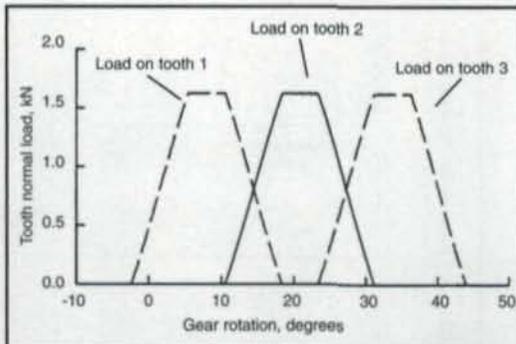

Figure 3—DANST computer program output of static gear tooth load, 68 N-m driver torque.

K_I increased as the load moved toward the tooth tip (load cases 12 to 7, Fig. 2b) due to the increased load lever arm. Loads on tooth 3 also produced tension at the crack tip, but at an order of magnitude less than those produced from the loads on tooth 2 (Fig. 2c). Loads on tooth 1 gave compression to the crack tip as shown by the negative K_I values (Fig. 2a).

Next, the actual load magnitudes on the gear tooth were considered as it went through the mesh. The computer program DANST (Dynamic ANalysis of Spur gear Transmission, Ref. 15) was used for the analysis. This program is based on a four-degree-of-freedom, torsional, lumped mass model of a gear transmission. The model includes driving and driven gears, connecting shafts, a motor, and a load. The equations of motion for this model were derived from basic gear geometry, elementary vibration principles, and time-varying tooth stiffnesses. For simplicity, the static gear tooth loads of the solution were determined (Fig. 3). These loads were determined from well-established gear tooth stiffness principles and static equilibrium. The loads are shown as a function of gear rotation for a driver torque of 68 N-m (599 in.-lb.). Tooth 2 began contact at a gear rotation of 10°. As the gear rotation increased, the load on tooth 2 gradually increased. Tooth 1 and tooth 2 shared the load for a rotation from 10° to 18°. From 18° to 23°, tooth 2 carried the complete load. At 23°, tooth 2 is considered at its highest point of single tooth contact (HPSTC).

The stress intensity factors as a function of gear rotation were then determined by multiplying the stress intensity factors determined from the units' loads (Fig. 2) by the actual tooth loads (Fig. 3) and applying superposition since linear elastic fracture mechanics was used. The results are shown in Figure 4. As expected, the mode I stress intensity factor (Fig. 4a) was mostly influenced by the load on tooth 2. Note that the largest value of K_I occurred at the HPSTC. Also note that

Paul A. Wawrzynek

is a senior research associate in the Computational Materials Institute at Cornell University's Theory Center and in the Cornell Fracture Group. A civil engineer, he has focused his research primarily on developing software for simulating crack growth in a range of engineering structures and materials. Also, he manages Fracture Analysis Consultants Inc., which provides crack growth analysis and software development services for different industries.

Anthony R. Ingraffea

is a professor at the School of Civil and Environmental Engineering at Cornell University, located in Ithaca, NY. A civil engineer, Ingraffea focuses his research on computer simulation and physical testing of complex fracturing processes. He and his students have performed research in using interactive computer graphics in computational fracture mechanics. With his students, he has written more than 180 papers on complex fracturing processes and computational fracture mechanics.

Robert F. Handschuh

is an aerospace engineer with the U.S. Army Research Laboratory at NASA's Glenn Research Center. His research has concentrated on power transmission; his research in gearing has focused on experimental and analytical studies of spiral bevel, face, and high-speed gearing. He has written or co-written more than 65 reports in the fields of seal, gear and numerical methods.
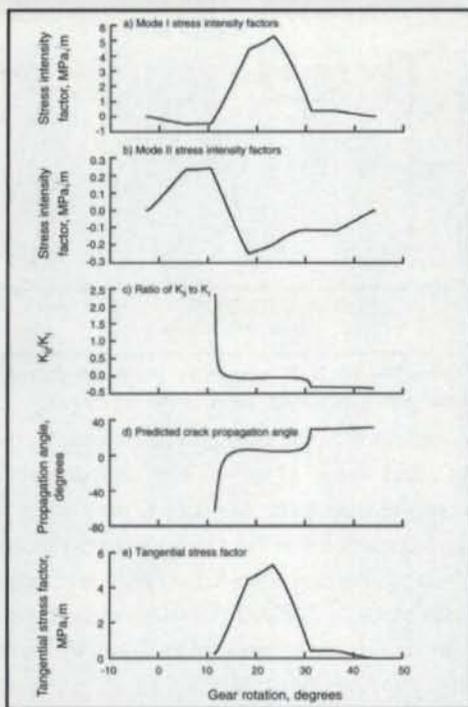
Figure 4—Stress intensity and tangential stress factors as a function of gear rotation, 68 N-m driver torque, 0.26 mm initial crack size.
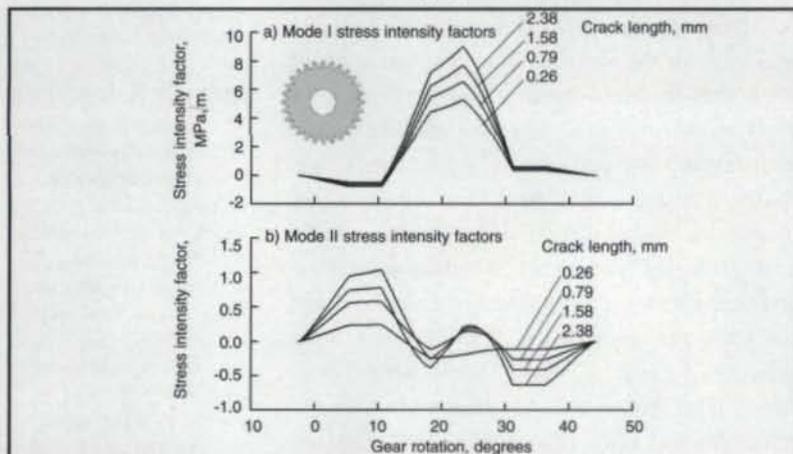

Figure 5—Stress intensity factors from gear tooth crack propagation simulation, backup ratio = 3.3.
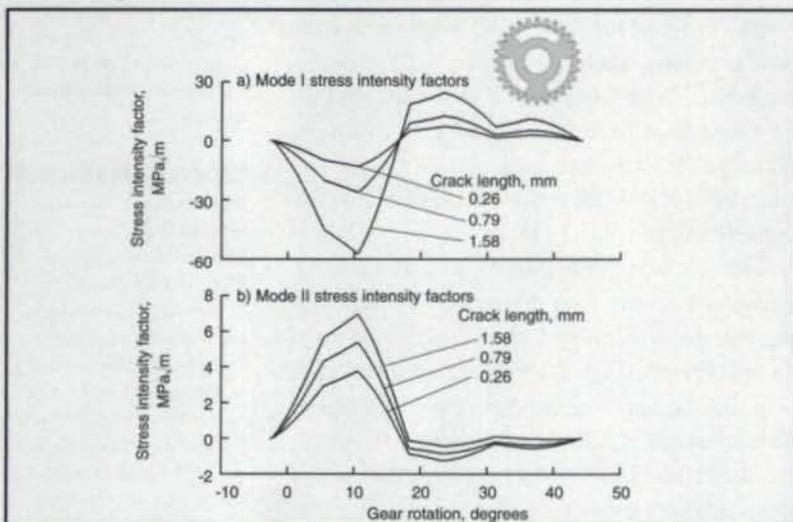

Figure 6—Stress intensity factors from gear tooth crack propagation simulation, backup ratio = 0.2.

the magnitude of K_I (Fig. 4a) was much larger than that of K_{II} (Fig. 4b). This implied that K_I was the driving force in the crack propagation. K_{II}, however, affected the crack propagation angle, as will be shown in the next section.

Crack Propagation Simulation. From Williams (Ref. 24), the tangential stress near a crack tip, $\sigma_{\theta\theta}$, is given by

$$\sigma_{\theta\theta} = \frac{1}{\sqrt{2\pi r}} \left(K_I \cos^3 \frac{\theta}{2} - 3K_{II} \sin \frac{\theta}{2} \cos^2 \frac{\theta}{2} \right) \quad (1)$$

where r and θ are polar coordinates with the origin at the crack tip. Erdogan and Sih (Ref. 8) postulated that crack extension starts at the crack tip and grows in the direction of the greatest tangential stress. The direction of the greatest tangential stress is determined by taking the derivative of Equation 1 with respect to θ, setting the expression equal to zero, and solving for θ. Performing the math, this predicted crack propagation angle, θ_m, is given by

$$\theta_m = 2 \tan^{-1} \left[\frac{\frac{K_I}{K_{II}} \pm \sqrt{\left(\frac{K_I}{K_{II}}\right)^2 + 8}}{4} \right] \quad (2)$$

From Equation 2, the predicted crack propagation angle is a function of the ratio of K_I to K_{II}. Erdogan and Sih (Ref. 8) used brittle plexiglass plates under static loading to validate their proposed theorems (i.e., the ratio of K_I to K_{II} was constant). For the gear problem in the current study, however, the ratio of K_I to K_{II} was not constant during gear rotation. This is shown in Figure 4c (actually plotted as the ratio K_{II} to K_I for clarity). In addition, Figure 4d gives the calculated θ_m from Equation 2 as a function of gear rotation.

In order to simulate gear crack propagation, a modification to the Erdogan and Sih theory was postulated in the current study. This modified theory states that the crack extension starts at the crack tip and grows in the direction of the greatest tangential stress as seen during engagement of the gear teeth. The procedure to calculate the crack direction is as follows:

1) K_I and K_{II} are determined as a function of gear rotation (Figs. 4a and 4b, as described in the previous section),

2) the ratio of K_I to K_{II} as a function of gear rotation is determined (Fig. 4c),

3) θ_m (using Eq. 2) as a function of gear rotation is determined (Fig. 4d),

4) $\sigma_{\theta\theta}$ (using Eq. 1) as a function of gear rotation is determined (Fig. 4e),

5) the predicted crack direction is the value of θ_m

for which $\sigma_{\theta\theta}$ is greatest during gear rotation.

For the gear example given, the tangential stress factor (defined as $\sigma_{\theta\theta}\sqrt{2\pi r}$) is plotted as a function of gear rotation in Figure 4e. This plot looks very similar to the mode I stress intensity factor plot (Fig. 4a) since K_I was much larger than K_{II} (see Eq. 1). The tangential stress was largest at the HPSTC (gear rotation of 23°) and the predicted crack propagation angle at this gear rotation was $\theta_m = 4.3°$.

Using this propagation angle, the crack was extended by 0.26 mm (0.010 in.), re-meshed, re-analyzed, and a new propagation angle was calculated using the method described above. This procedure was repeated a number of times to produce a total crack length of 2.38 mm (0.094 in.). The 0.26-mm crack extension length was based on prior experience in order to produce a smooth crack path. Figure 5 shows the stress intensity factors versus gear rotation for a number of crack lengths. Note that the mode I stress intensity factors looked similar but with increased magnitude as the crack length increased. In all cases, the selected crack propagation angles occurred when the tooth load was placed at the HPSTC. Figure 6 shows a similar analysis but with a model of a thin-rimmed gear. Here, the gear was modeled based on the previous design, but with slots incorporated in the rim to simulate a thin-rimmed gear. The backup ratio for this model was 0.2. As seen, the magnitudes of the mode I stress intensity factors during tension (gear rotations 18° to 45°) were larger than that of the 3.3 backup ratio gear. Also, there was a significant increase in the compressive K_I (gear rotation less than 18°) due to the increased compliance of the thin rim gear.

Comparison to Experiments. Figure 7 shows the results of the analysis compared to experimental tests in a gear fatigue apparatus. The original model (backup ratio of 3.3), as described before, was compared along with models of backup ratio of 1.0 and 0.3. These later two models were created using slots in the gear blank, as previously described. The experiments were first reported by Lewicki and Ballarini (Ref. 13). Here, notches were fabricated in the tooth fillet region to initiate tooth cracking of test gears of various rim thicknesses. The gears were run at 10,000 rpm and at a variety of increasing loads until tooth or rim fracture occurred. As seen from the figure, good correlation of the predicted crack trajectories to experimental results was achieved. For backup ratios of 3.3 and 1.0, tooth fractures occurred. For the backup ratio of 0.3, rim fracture occurred.

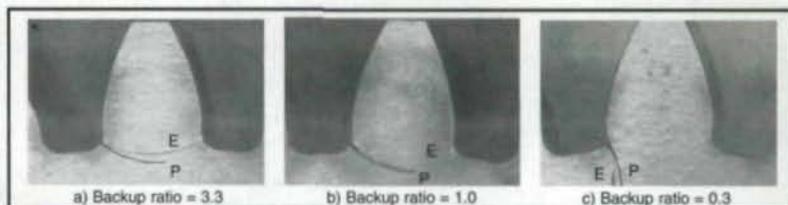As a final note, the analysis indicated that the

Figure 7—Comparison of predicted gear tooth crack propagation paths with experimental results (P = predicted, E = experiments).
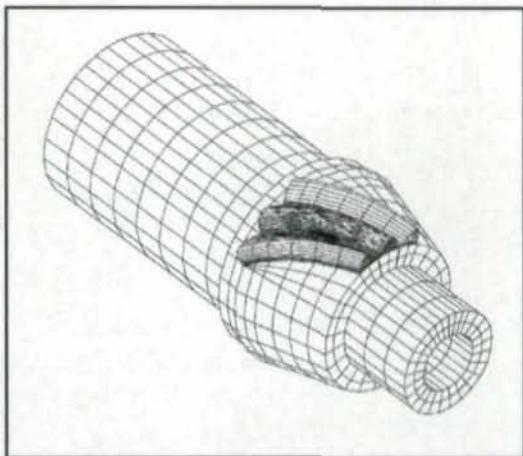

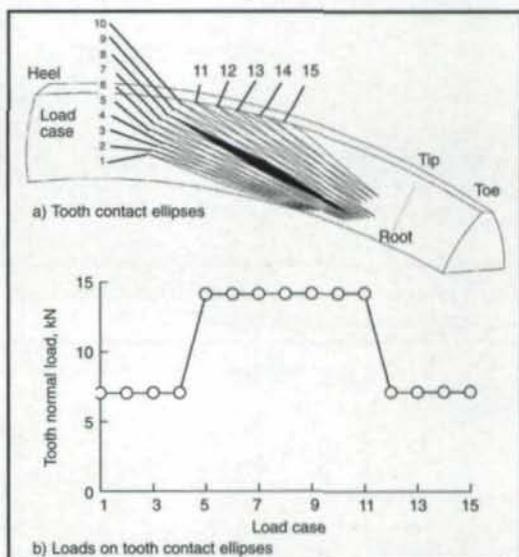*Figure 8—Boundary element model of OH-58 spiral-bevel pinion.*

Figure 9—Location of tooth contact ellipses and magnitude of load on OH-58 spiral-bevel pinion tooth.

maximum tangential stress at the crack tip always occurred when the tooth load was positioned at the HPSTC. Thus, for two-dimensional analysis, crack simulation based on calculated stress intensity factors and mixed mode crack angle prediction techniques can use a simple static analysis in which the tooth load is located at the HPSTC. This was based on a modification to the Erdogan and Sih crack extension theory and the fact that the mode I stress intensity factor was much larger than the mode II factor.

Three-Dimensional Analysis

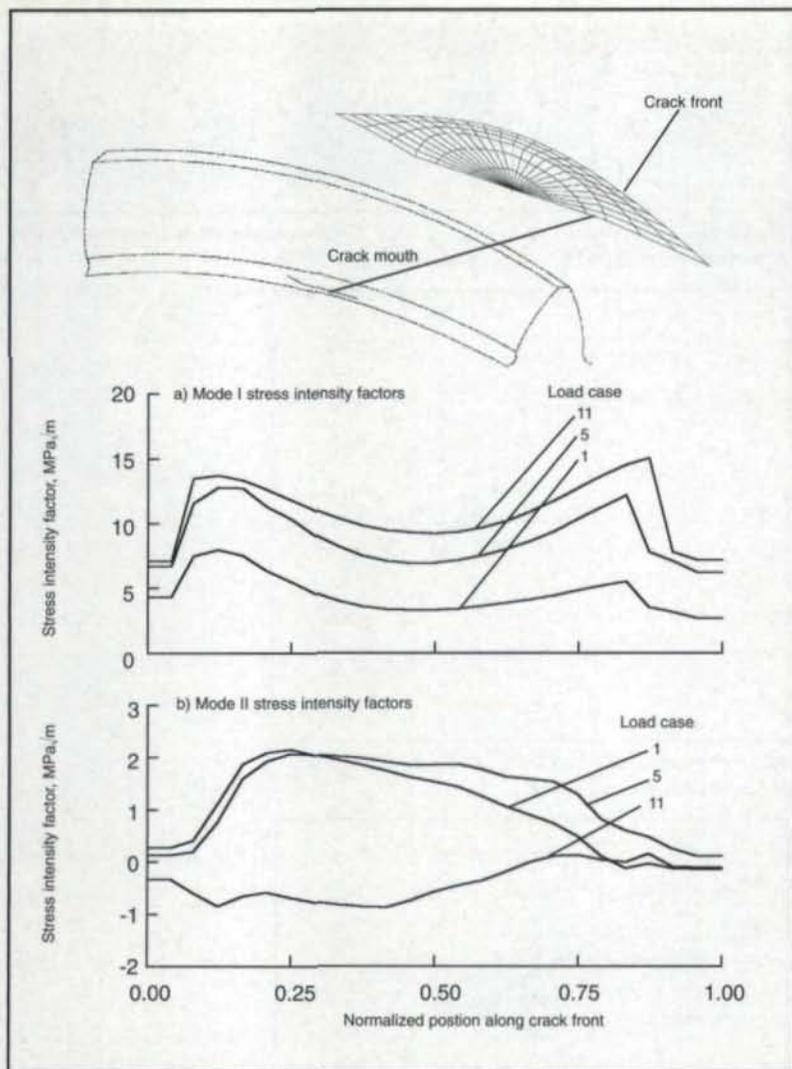***Gear Modeling.*** The three-dimensional analy-

Figure 10—Stress intensity factors from three-dimensional OH-58 pinion tooth crack propagation simulation; step 1, crack area = 5.96 mm².
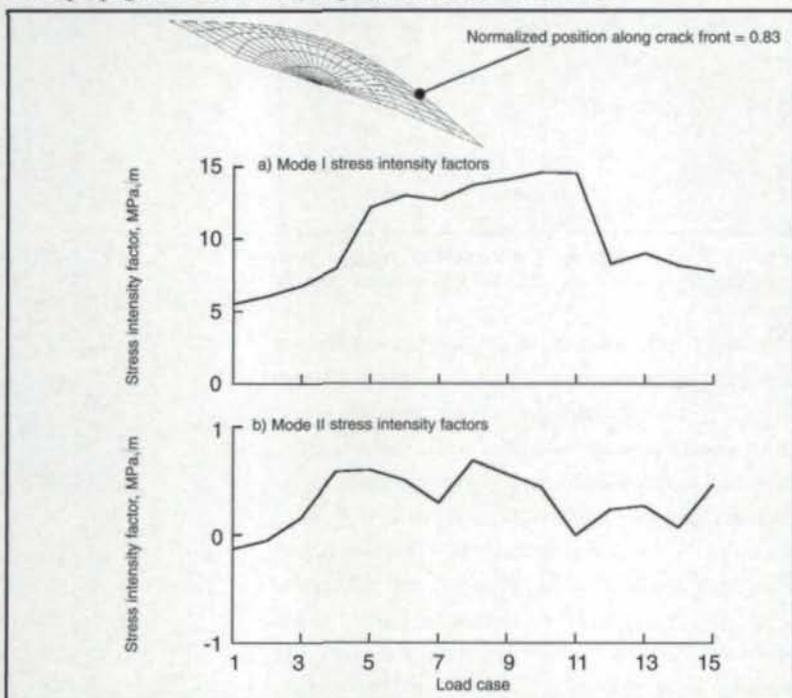

Figure 11—Stress intensity factors from three-dimensional OH-58 pinion tooth crack propagation simulation; step 1, normalized position along crack front = 0.83.

sis was performed using the FRANC3D (FRacture ANalysis Code for 3 Dimensions) computer program developed by Wawrzynek (Ref. 23). This program uses boundary element modeling and principles of linear elastic fracture mechanics to analyze cracked structures. The geometry of three-dimensional structures with non-planar, arbitrary shaped cracks can be modeled. The modeling of a three-dimensional cracked structure is performed through a series of programs. Structure geometry grid point data are imported to a solid modeler program. Here, appropriate curves and faces (or patches) are created from the grid data, as well as a closed-loop surface geometry model. This surface model is then imported to the FRANC3D program for boundary element model preparation. The user can then mesh the geometry model using 3- or 6-node triangular surface elements, or 4- or 8-node quadrilateral elements. Boundary conditions (applied tractions and prescribed displacements) are applied on the model geometry over faces, edges, or points. Initial cracks, such as elliptical or penny shaped, can be inserted in the structure. After complete formulation, the model is shipped to a boundary element equation solver program. Once the displacement and traction unknowns are solved, the results are exported back to the FRANC3D program for post-processing. Fracture analysis, such as stress intensity factor calculations, can then be performed.

The spiral-bevel pinion of the OH-58C helicopter main rotor transmission was modeled to demonstrate the three-dimensional analysis. The pinion had 19 teeth, a 20° pressure angle, a 30° mean spiral angle, a module of 3.66 mm (diametral pitch of 6.94/in.), and a face width of 32.51 mm (1.28 in.). For OH-58 operation, the pinion mates with a 71-tooth spiral-bevel gear, operates at 6,060 rpm, and has a design torque of 350 N-m (3,099 in.-lbs.).

The boundary element model of the OH-58 pinion developed by Spievak (Ref. 22) was used for the study. Three teeth, the rim cone, and the bearing support shafts were modeled (Fig. 8). The tooth surface and fillet coordinates were determined from the methods developed by Handschuh and Litvin (Ref. 11) and Litvin and Zhang (Ref. 16). The mesh of the three teeth was refined for improved accuracy. A half-ellipse initial crack with major and minor diameters of 3.175 mm and 2.540 mm, respectively (0.125 in. and 0.100 in.), was placed in the fillet of the middle tooth normal to the surface. The crack was centered along the face width and centered along

the fillet. The complete gear model had a total of about 2,600 linear elements (both triangular and quadrilateral) and about 2,240 nodes. For boundary conditions, the end nodes of the larger-diameter shaft were fixed and the nodes on the outer diameter of the smaller-diameter shaft were constrained in the radial directions. Again, the material was steel.

Tooth Contact Analysis and Loading Scheme. Due to the geometrical complexities and three-dimensional action, numerical methods are required to determine the contact loads and positions on spiral-bevel teeth since no closed-form solution exists. The method of Litvin and Zhang (Ref. 16) was used to determine the mean contact points on the spiral-bevel pinion tooth. The method modeled tooth generation and tooth contact simulation of the pinion and gear. With the mean contact points taken as the centers, contact ellipses were determined using Hertzian theory (Ref. 10). Figure 9 shows the estimated contact ellipses on the spiral-bevel pinion tooth. Fifteen separate ellipses (load cases) were determined, starting from the root of the pinion and moving toward the tooth tip and toe. Load cases 1–4 and 12–15 were double tooth contact regions while load cases 5–11 were single tooth contact regions. Note that load case 11 corresponds to the load at the HPSTC. For each load case using the boundary element method, tractions were applied normal to the surface, to the appropriate ellipse with the magnitude equal to the tooth normal force divided by the ellipse area.

Crack Propagation Simulation. The procedure for the three-dimensional crack propagation simulation of the OH-58 spiral-bevel pinion was as follows. For each of the load cases of Figure 9, the mode I and mode II stress intensity factors were determined at 25 points along the crack front (note that for three-dimensions, there is a crack front, not just a crack tip as in two-dimensions). The extended crack directions at each of these 25 points were determined using the modified Erdogan and Sih crack extension theory as described in the two-dimensional analysis. That is, as the cracked spiral-bevel pinion tooth was engaged in the mesh, the crack extension started at each point along the crack front and grew in the direction of the greatest tangential stress at those points during mesh. The amount of crack extension at each point along the crack front was determined based on the Paris crack growth relationship (Ref. 18) where

$$a_i = a_{max}\left(\frac{K_{I,i}}{K_{I,max}}\right)^n \qquad (3)$$

Table I—Results of multiple load case crack simulation analysis.

Step	Crack area (mm²)	Crack front point(s)	Load case for largest $\sigma_{\theta\theta}$
0	3.12	1	8
		2–25	11
1	5.96	1	9
		2,4–7, 21, 23–25	10
		3,8–20, 22	11
2	10.35	1	10
		2–25	11
3	13.35	7, 9, 20	8
		5, 6, 10–15, 21, 26, 27	9
		1–4, 8, 16–19, 22–25	11

where a_i was the amount of extension of the i_{th} point along the crack front, $K_{I,i}$ was the mode I stress intensity factor of the i_{th} point along the crack front corresponding to the load case which gave the largest tangential stress for that front point, $K_{I,max}$ was the value of the largest $K_{I,i}$ along the crack front, a_{max} was the maximum defined crack extension along the crack front, and n was the Paris material exponent. From experience, the maximum extension size, a_{max}, was set to 1.27 mm (0.050 in.). The Paris exponent, n, was set to 2.954 based on material tests for AISI 9310 steel by Au and Ke (Ref. 4). A third-order polynomial was then used to smooth the extended crack front. The new crack geometry was then re-meshed. After re-meshing, the model was rerun and solved for stress intensity factors and crack propagation directions. The above procedure was repeated a number of times to simulate crack growth in the gear tooth.

Table I gives results from the first four steps during this process. Note that step 0 corresponds to the initial half-ellipse crack. For steps 0 and 2, the largest tangential stress occurred at the HPSTC (load case 11) for the majority of the points along the crack front. For steps 1 and 3, the largest tangential stress occurred at load cases 8, 9, 10, or 11.

As previously stated, the mode I and mode II stress intensity factors were determined at 25 points along the crack front. This was true for steps 0 through 2. For step 3, however, the mode I and mode II stress intensity factors were determined at 27 points along the crack front. This was due to the way the FRANC3D program extended the crack surface of the third step. For steps 0 through 2, the crack front was a member of one continuous geometry face (FRANC3D defines a geometry face as a 3- or 4-sided surface.) For
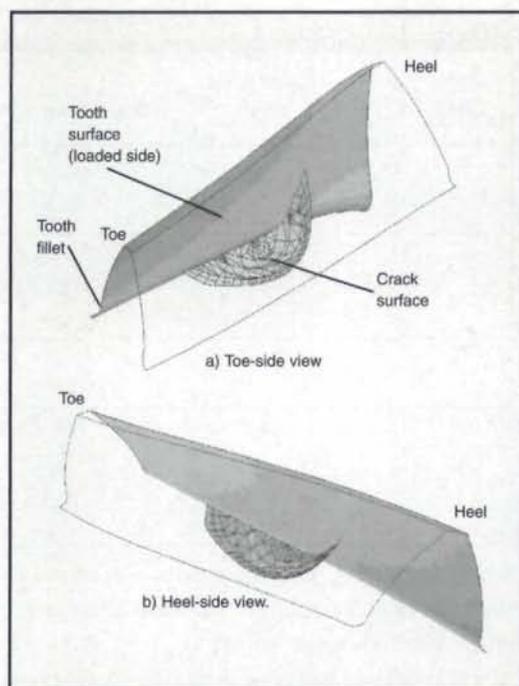
Figure 12—OH-58 spiral-bevel pinion tooth crack propagation simulation after seven steps.
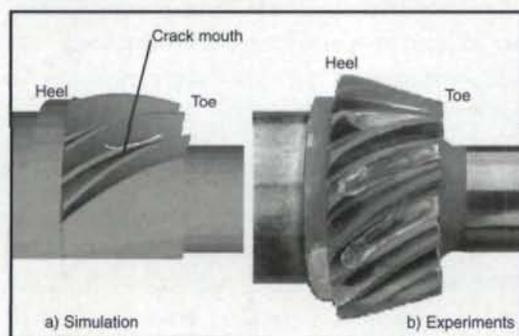

Figure 13—Comparison of OH-58 spiral-bevel pinion tooth crack propagation simulation to experiments.

step 3, the crack front was a member of three adjacent geometry faces, thus producing 27 points along the crack front.

Figure 10 shows the stress intensity factor distribution along the crack front for step 1 (crack area of 5.96 mm² (0.009 in.²)). Similar to the spur gear analyses, K_I was larger as the load moved from the root to the tip due to the larger load lever arm. Other than absolute magnitude, the K_I distributions along the crack front looked similar for the various load cases. Figure 11 depicts the stress intensity factors plotted against load case (at a point along the front, biased toward the toe, normalized position along the crack front of 0.83) This figure shows the simulated distribution as the pinion engages in mesh with the gear. Note again that the ratio of K_{II} to K_I was not constant during engagement.

Figure 12 shows exploded views of the pinion crack simulation after seven steps. It should be noted that the loading was placed only at the HPSTC for the last three steps. This was due to modeling difficulties encountered using the multi-load analysis. It was felt that this simplification did not significantly affect the results due to the smoothing curve-fit used. In addition, the tangential stress near the crack tip was either largest, or near its largest value, when the load was placed at the HPSTC.

Comparison to Experiments. Figure 13 shows the results of the analysis compared to experimental tests. The experimental tests were performed in an actual helicopter transmission test facility. As was done with the gear fatigue tests described before, notches were fabricated in the fillet of the OH-58 pinion teeth to promote fatigue cracking. The pinion was run at full speed and with a variety of increasing loads until failure occurred. Shown in the figure are three teeth that fractured from the pinion during the tests (Fig. 13b). Although the notches were slightly different in size, the fractured teeth had basically the same shape.

A side view of the crack propagation simulation is shown in Figure 13a for comparison to the photograph of the tested pinion in Figure 13b. From the simulation, the crack immediately tapered up toward the tooth tip at the heel end. This trend matched that seen from the tests. At the toe end, the simulation showed the crack progressing in a relatively straight path. This also matched the trend from the tests. Toward the latter stages of the simulation, however, the crack tended to taper toward the tooth tip at the toe end. This did not match the tests. One problem encountered in the simulation during the later steps was that the crack at the heel end of the tooth became close to the actual contact ellipses. It was felt that the crack-contact interaction may have influenced the trajectory predictions to cause the discrepancy.

Spievak (Ref. 22) reported on another method to account for the non-uniform K_{II} to K_I ratio during pinion tooth engagement. This method considered contributions from all load cases in the crack angle prediction scheme and presented a method to accumulate the load effects. From these studies, reported crack propagation simulation of an OH-58 pinion also predicted the erroneous taper toward the tooth tip at the toe end. Again, the crack-contact interaction may have influenced the trajectory predictions to cause the discrepancy. Spievak also reported on a simulation using only the load at the HPSTC. The crack trajectories from that simulation were similar to the trajectories in the current study. It should be

noted that the proposed method in the current study to account for moving tooth loads for the three-dimensional analysis was extremely cumbersome. It is therefore felt that the analysis using only the load at the HPSTC appeared accurate as long as the crack did not approach the contact region on the tooth.

Conclusions

A study to determine the effect of moving gear tooth load on crack propagation predictions was performed. Two-dimensional analysis of an involute spur gear using the finite element method was investigated. Also, three-dimensional analysis of a spiral-bevel pinion gear using the boundary element method was discussed. The following conclusions were derived:

1) A modified theory for predicting gear crack propagation paths based on the criteria of Erdogan and Sih was validated. This theory stated that as a cracked gear tooth was engaged in mesh, the crack extension started at the crack tip and grew in the direction of the greatest tangential stress during mesh.

2) For two-dimensional analysis, crack simulation based on calculated stress intensity factors and mixed mode crack angle prediction techniques can use a simple static analysis in which the tooth load is located at the highest point of single tooth contact.

3) For three-dimensional analysis, crack simulation can also use a simple static analysis in which the tooth load is located at the highest point of single tooth contact as long as the crack does not approach the contact region on the tooth. ○

References

1. Abersek, B. and J. Flasker, "Stress Intensity Factor for Cracked Gear Tooth," *Theoretical and Applied Fracture Mechanics*, 1994, Vol. 20, No. 2, pp. 99–104.
2. Abersek, B. and J. Flasker, "Experimental Analysis of Propagation of Fatigue Crack on Gears," *Experimental Mechanics*, 1998, Vol. 38, No. 3, pp. 226–230.
3. Arikin, M.A., A.I. Tarhan, and O.S. Yahoj, "Life Estimate of a Spur Gear with a Tooth Cracked at Fillet Region," Proceedings of the ASME Design Engineering Technical Conference, 1998, Atlanta, GA.
4. Au, J.J. and J.S. Ke, "Correlation Between Fatigue Crack Growth Rate and Fatigue Striation Spacing in AISI 9310 (AMS 6265) Steel," *Fractography and Material Science, ASTM STP 733*, 1981, pp. 202–221.
5. Blarasin, A., M. Guagliano and L. Vergani, "Fatigue Crack Growth Predictions in Specimens Similar to Spur Gear Teeth," *Fatigue & Fracture of Engineering Materials & Structures*, 1997, Vol. 20, No. 8, pp. 1171–1182.
6. Ciavarella, M. and G. Demelio, "Numerical Methods for the Optimization of Specific Sliding, Stress Concentration, and Fatigue Life of Gears," *International Journal of Fatigue*, 1999, Vol. 21, No. 5, pp. 465–474.
7. Curtin, T.J., R.A. Adey, J.M.W. Baynham and P. Marais, "Fatigue Crack Growth Simulation for Complex Three-Dimensional Geometry and Loading," Proceedings from the 2nd Joint NASA/FAA/DOD Conference on Aging Aircraft, 1998, Williamsburg, VA.
8. Erdogan, F. and G.C. Sih, "On the Crack Extension in Plates Under Plane Loading and Transverse Shear," *Journal of Basic Engineering*, 1963, Vol. 85, pp. 519–527.
9. Glodez, S., S. Pehan, and J. Flasker, "Experimental Results of the Fatigue Crack Growth in a Gear Tooth Root," *International Journal of Fatigue*, 1998, Vol. 20, No. 9, pp. 669–675.
10. Handschuh, R.F. and T.P. Kicher, "A Method for Thermal Analysis of Spiral Bevel Gears," *Journal of Mechanical Design*, 1996, Vol. 118, No. 4, pp. 580–585.
11. Handschuh, R.F. and F.L. Litvin, "A Method for Determining Spiral-Bevel Gear Tooth Geometry for Finite Element Analysis," NASA TP-3096, AVSCOM TR-91-C-020, 1991.
12. Inoue, K. and M. Kato, "Crack Growth Resistance Due to Shot Peening in Carburized Gears," Presented at the 30th AIAA/ASME/SAE/ASEE Joint Propulsion Conference, 1994, Indianapolis, IN.
13. Lewicki, D.G. and R. Ballarini, "Effect of Rim Thickness on Gear Crack Propagation Path," *Journal of Mechanical Design*, 1997, Vol. 119, No. 1, pp. 88–95.
14. Lewicki, D.G., A.D. Sane, R.J. Drago, and P.A. Wawrzynek, "Three-Dimensional Gear Crack Propagation Studies," Proceedings of the 4th World Congress on Gearing and Power Transmission, Paris, France, 1999, Vol. 3, pp. 2311–2324.
15. Lin, H.H., R.L. Huston and J.J. Coy, "On Dynamic Loads in Parallel Shaft Transmissions: Part I - Modeling and Analysis," *Journal of Mechanisms, Transmissions, and Automation in Design*, 1988, Vol. 110, No. 2, pp. 221–225.
16. Litvin, F.L. and Y. Zhang, "Local Synthesis and Tooth Contact Analysis of Face-Milled Spiral Bevel Gears," NASA Contractor Report 4342, AVSCOM Technical Report 90-C-028, 1991.
17. Nicoletto, G. "Approximate Stress Intensity Factors for Cracked Gear Teeth," *Engineering Fracture Mechanics*, 1993, Vol. 44, No. 2, pp. 231–242.
18. Paris, P.C. and F. Erdogan, "A Critical Analysis of Crack Propagation Laws," *Journal of Basic Engineering*, 1963, Vol. 85, pp. 528–534.
19. Pehan, S., T.K. Hellen, J. Flasker and S. Glodez, "Numerical Methods for Determining Stress Intensity Factors vs. Crack Depth in Gear Tooth Roots," *International Journal of Fatigue*, 1997, Vol. 19, No. 10, pp. 677–685.
20. Rice, J.R. "A Path Independent Integral and the Approximate Analysis of Strain Concentration by Notches and Cracks," *Journal of Applied Mechanics*, 1968, Vol. 35, pp. 379–386.
21. Sfakiotakis, V.G., D.E. Katsareas and N.K. Anifantis, "Boundary Element Analysis of Gear Teeth Fracture," *Engineering Analysis with Boundary Elements*, 1997, Vol. 20, No. 2, pp. 169–175.
22. Spievak, L.E. "Simulating Fatigue Crack Growth in Spiral Bevel Gears," Masters of Science Thesis, Cornell University, 1999.
23. Wawrzynek, P.A. "Discrete Modeling of Crack Propagation: Theoretical Aspects and Implementation Issues in Two and Three Dimensions," Ph.D. Dissertation, Cornell University, 1991.
24. Williams, M.L. "On the Stress Distribution at the Base of a Stationary Crack," *Journal of Applied Mechanics*, 1957, Vol. 24, No. 1, pp. 109–114.